# Towards the Integration of Terrestrial and Non-Terrestrial Networks: a Testbed for in-Lab Evaluation

Enrico Boffetti*†‡, Salvatore Carbonara*†‡, Daniele Pugliese*†‡, Giovanni Grieco*,
Carolina Sbiroli*, Alessio Fascista*†, Arcangela Rago*†, Giuseppe Piro*†
*Dept. of Electrical and Information Engineering, Politecnico di Bari, Bari, Italy
†CNIT, Consorzio Nazionale Interuniversitario per le Telecomunicazioni, Italy

***Abstract*—The integration of Terrestrial and Non-Terrestrial Networks (T/NTNs) is expected to be a native capability of the Sixth-Generation (6G) of mobile networks. Driven by the growing demand for reliable and ubiquitous connectivity, recent Fifth-Generation (5G) releases have already begun addressing some of the challenges in developing a three-dimensional (3D) architecture combining T/NTN. In this context, this work presents a preliminary experimental evaluation of integrated 5G T/NTN scenarios, enabled by a laboratory testbed currently under development within the RESTART ITA-NTN project. The testbed allows for the emulation of ground-, aerial-, and satellite-based links interfacing with 5G Radio Units (RUs) through advanced Radio Frequency (RF) channel modeling and emulation. After an overview of the 5G Next Generation Radio Access Network (NG-RAN) and the specific adaptations required to support NTN scenarios, the main integrated T/NTN architectures are outlined. To assess these architectures and emulate T/NTN scenarios under controlled conditions, the testbed integrates commercial Software Defined Radios (SDRs) platforms with the Keysight F8820A PROPSIM FS16 channel emulator to replicate several customisable channel conditions, using the OpenAirInterface (OAI) stack for full 5G NG-RAN and core functionality. Preliminary evaluations of the considered T/NTN scenarios are carried out, highlighting key operational characteristics and selected performance metrics, offering insights into challenges and opportunities of extending 5G capabilities to NTN platforms.**

***Index Terms*—Sixth-Generation, Integrated Terrestrial/Non-Terrestrial Networks, Channel Emulator**

## I. Introduction

Terrestrial Networks (TNs) have historically served as the backbone of our digital lives, but their inherent dependencies on geographical constraints and susceptibility to localised disruptions highlight a critical need for enhanced resilience, expanded coverage, and unparalleled reliability. To address these limitations, Fifth-Generation (5G) and beyond networks are evolving strategically, driven by a transformative paradigm that will be fully realised in the Sixth-Generation (6G) of mobile networks: the convergence of TNs and Non-Terrestrial Networks (NTNs), aimed at enabling intelligent and pervasive connectivity across heterogeneous environments [1].

The vision of a fully integrated Three-Dimensional (3D) communication infrastructure, where satellites, High Altitude Platforms (HAPs), and aerial vehicles seamlessly complement the ground-based infrastructure, holds the potential to unlock unprecedented levels of global reach, capacity, and service continuity. Such integrated Terrestrial and Non-Terrestrial Network (T/NTN) architectures are not merely an evolution but a fundamental shift, poised to bridge digital divides, enable critical communications in disaster-stricken areas, and empower new classes of applications [2], [3].

Among the various orbital configurations of satellite-based network nodes, those belonging to the Low Earth Orbit (LEO) and Geostationary Earth Orbit (GEO) categories are primarily considered in the latest Third Generation Partnership Project (3GPP) releases [4]. Specifically, GEO satellites provide extensive coverage over vast regions. However, they are subject to substantial propagation delays and must be supported by bulky ground infrastructure, including high-directivity antennas and high-power signal amplifiers. Conversely, LEO satellites are typically organised into numerous constellations to ensure global coverage, whilst facing challenges such as frequent handovers and channel-related effects (e.g., Doppler shift) [5].

Even in the current phase of 5G development, experimental evaluation of NTN architectures is essential to assess their feasibility in real-world scenarios and to validate the protocol adaptations introduced by 3GPP for enabling integrated T/NTNs [6]. However, the effective employment of space infrastructures, as demonstrated in [7], remains challenging without direct involvement from aerospace stakeholders. A practical alternative is the use of dedicated hardware and software to build lab-scale benchmarks for both GEO and LEO scenarios [8]–[10]. For the 5G protocol stack part, OpenAirInterface (OAI) is usually preferred among the other solutions due to its flexibility and adherence with 3GPP Release-17 and beyond specifications [11]. On the radio side, Software Defined Radios (SDRs) provide a powerful and reconfigurable platform for implementing the Radio Access Network (RAN). Yet, when large-scale or high-fidelity scenarios must be emulated, SDRs alone are insufficient; a hardware channel emulator is required to introduce realistic channel impairments and manipulate RF signals accordingly. This hybrid approach ensures higher realism than system-level simulations by accounting for hardware non-idealities.

This work presents the ongoing efforts undertaken in the context of the RESTART ITA-NTN project, where a set of promising integrated 5G T/NTNs architectures has been defined. To experimentally evaluate them, a dedicated laboratory testbed has been designed and implemented. Building on existing contributions where similar setups have been proposed, our work provides a more comprehensive characterization of the in-lab experimental testbed, encompassing in detail both

‡The first three authors contributed equally to this work.

hardware and software components. The proposed framework enables the analysis of a combined architecture where T/NTNs and 5G elements operate cooperatively. Furthermore, a preliminary performance evaluation of the TN and NTN segments is presented, offering insights into the technical challenges and potential opportunities arising from their integration.

## II. From 5G-NTNs to Integrated T/NTNs

Starting from Release 17, 3GPP has introduced several updates to the 5G New Radio (NR) specifications to support aerial and space nodes within the Next Generation Radio Access Network (NG-RAN). This section provides an overview of the key enhancements introduced. Building on these developments, a set of integrated T/NTNs architectures are identified, each tailored to support specific use cases.

### *A. 5G-NTN Overview*

As a step toward 6G, the current generation has begun integrating NTN nodes, such as LEO, Medium-Earth Orbit (MEO), and GEO satellites, Unmanned Aerial Vehicles (UAVs), and High Altitude Platform Systems (HAPSs), to extend coverage, enhance resilience, and support advanced use cases in underserved or challenging environments [2]. UAVs, for example, can act as agile access nodes for rapid deployment in emergencies or large-scale events. To enable such integration, the 5G architecture has evolved to support heterogeneous connectivity through virtualization, functional disaggregation, and standardised interfaces

Focusing on the NG-RAN only, the interoperability with each NTN platform brings several challenges, summarised in (i) higher delays which affect Automatic Repeat Request (ARQ) procedures, (ii) large Doppler shifts that degrade or disrupt decoding capabilities, and (iii) erratic network access availability. To cope with these issues, several adaptations have been introduced in the latest 3GPP specifications. At the physical layer, the modifications aim to support time-variant propagation delays and frequency offset, compensating them via continuous frequency offset and timing drift estimation. At the Media Access Control (MAC) layer, adaptations target retransmission strategies and resource management. For GEO satellites, Hybrid Automatic Repeat reQuest (HARQ) is typically disabled to avoid inefficiencies due to long delays, while LEO systems can support up to 32 HARQ processes to handle dynamic link conditions. Modifications have also been introduced to the Timing Advance (TA) and Random Access (RA) procedures to ensure proper synchronization in NTN scenarios. Additional enhancements involve Channel State Information (CSI) reporting, Adaptive Modulation and Coding (AMC), and handover mechanisms, particularly critical for LEO platforms. At the Radio Link Control (RLC) and Packet Data Convergence Protocol (PDCP) layers, larger ARQ buffers, extended sequence numbers, and longer reassembly timers have been introduced to accommodate higher latencies. Similarly, the Radio Resource Control (RRC) layer supports extended UE timers (T300, T301, T311) to maintain robust connection procedures under significant propagation delays. Many of these parameters can be configured at the UE via System Information Block (SIB) 19, which includes satellite access settings, timing advance values, and other NTN-specific broadcast information [4].

From a functional perspective, non-terrestrial nodes can extend the NG-RAN in either transparent or regenerative mode. In transparent mode, the node acts as a passive radio relay, simply forwarding signals between the User Equipment (UE) and the NTN Gateway (GW) without protocol-layer processing. Intelligence and control remain entirely ground-based, typically at a terrestrial gateway, allowing the RAN to operate without major architectural changes [12]. In contrast, regenerative mode enables the non-terrestrial node (e.g., a satellite or UAV) to host parts of the RAN stack, up to the MAC or even the RLC/PDCP layer. This allows for localised signal processing and autonomous radio resource management, reducing latency effects and enabling link optimisation. While not explicitly covered in current 3GPP specifications, regenerative architectures also open the door to Inter-Satellite Link (ISL) integration. Implementing regenerative mode requires higher onboard computational capabilities, robust synchronization, and seamless coordination with the core network. It is particularly suited for mission-critical services, Ultra-Reliable-Low-Latency Communication (URLLC) in remote areas, and high-density UE scenarios [13].

### *B. Envisioned Integrated T/NTN Architectures*

The integration of NTN nodes into existing TN infrastructures enables the design of architectures in which TN and NTN nodes can jointly provide network services to UE. This extends coverage and provides a highly resilient network maintaining ubiquitous connectivity. In the following, some promising architectures for T/NTNs are presented [2].

*UAV-based Relaying*: In this architecture, the mobility of UAVs is crucial for extending the coverage of TNs. UAVs can provide temporary connectivity in areas affected by network failures, natural disasters, or at cell edges where users typically experience poor service. Depending on their payload capabilities, UAVs may operate in either transparent or regenerative modes, acting as simple relays or as fully functional 5G Node Bs (gNBs), respectively. A major challenge lies in payload and battery limitations: indeed, UAVs typically cannot carry heavy equipment, and communication modules are energy-intensive, requiring frequent recharging and restricting flight duration.

*Satellite-Based Relaying*: The satellite-based relaying architecture can serve ground-based UEs through direct access or support terrestrial infrastructure via backhaul links (indirect access). Specifically, in direct access, the satellite may operate in both transparent and regenerative mode, with the same functionalities seen for the UAV-based relaying. Regarding indirect access, the paradigm Integrated Access Backhaul (IAB) can be integrated to improve backhaul connections in challenging environments using wireless links, instead of classical cable infrastructures [14]. This approach can improve coverage and network services in areas that are inaccessible to traditional TN infrastructures. The primary limitations of this architecture include propagation delays, especially in the case of GEO satellites due to their high orbital altitude, which results in elevated Round Trip Time (RTT) values for communications. Conversely, LEO satellites, while offering

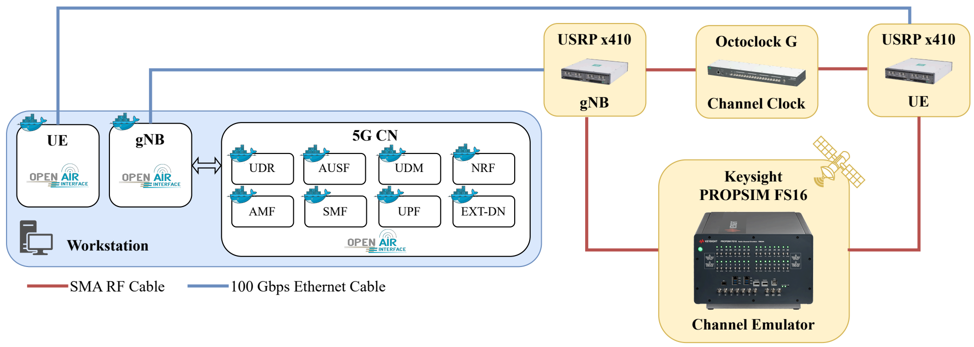


Fig. 1. Comprehensive representation of the proposed testbed for emulating integrated T/NTN scenarios, including key software and hardware components.

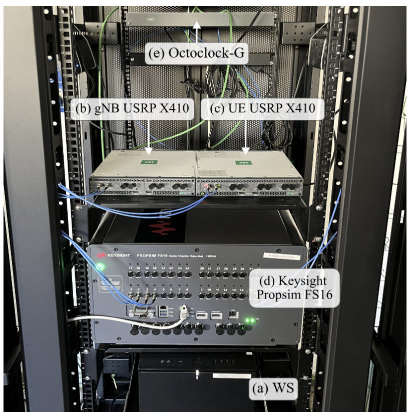


Fig. 2. Hardware setup for the experimental evaluation of integrated T/NTNs.

lower latency, introduce notable Doppler effects due to their relative motion with respect to ground-based UEs. In addition, atmospheric conditions can further degrade communication quality, intensifying propagation losses associated with long transmission distances.

*3D Single-Connectivity*: By combining the UAV-based relaying and satellite-based architectures, it is possible to obtain a 3D architecture in which NTN elements with a lower altitude can relay communications to NTNs at higher altitude, so reducing latency and improving the network performance via intermediate aerial nodes. Furthermore, all the NTN nodes involved can work in a transparent or regenerative mode, enabling different configurations. However, this type of architecture also introduces significant interoperability challenges, particularly when integrating heterogeneous NTN elements. In addition, the single-connectivity configuration is inherently more vulnerable to service disruptions caused by network failures or congestion events, such as the loss of connectivity due to node malfunctions or outages.

*3D Multi-Connectivity*: This architecture aims at fully integrating both the TN and NTN infrastructures. Specifically, UEs can connect to both the TN and NTN segments, or even to two separate NTN segments, the latter requiring ISLs to handle inter-satellite communication. In this architecture, the network assigns a Master Node and a Secondary Node, with the UE connected to both, while all traffic flows through the Master Node. When link quality degrades, the network dynamically reselects the nodes to maintain service continuity. By leveraging multi-connectivity, UEs benefit from seamless handovers across network segments, ensuring uninterrupted connectivity even during failures. The architecture also supports flexible configurations, accommodating NTN components operating in both transparent and regenerative modes.

## III. A Testbed for Integrated T/NTN Emulation

This section describes the proposed testbed for analysing 5G-based integrated T/NTNs. In particular, the aim is to provide emulation capabilities for both a TN and an NTN segment. Fig. 1 provides a schematic view of the complete hardware and software setup. In the following, we describe each testbed component in detail.

### *A. Hardware Components*

Hardware components are organised in a server rack within the experimental Laboratory of Integrated Terrestrial and Non-Terrestrial Networks and Services (iTNT-NS), realised as part of the RESTART Program at the Politecnico di Bari (Italy), as shown in Fig. 2. From a computing perspective, the setup features a workstation (WS) running Ubuntu 24.04 LTS, labeled as (a) in Fig. 2, equipped with an AMD Ryzen Threadripper PRO 5965WX processor, an NVIDIA GeForce RTX 4070 Ti GPU, and 128 GB of DDR4 RAM. As with most 5G in-lab implementations, our testbed leverages SDR technology to realise the Radio Frequency (RF) front-end. Specifically, two NI Ettus Universal Software Radio Peripheral (USRP) X410 devices, labeled (b) and (c) in Fig. 2, are employed. The former is controlled by the WS to operate as a 5G gNB, while the latter acts as a 5G UE. The WS interfaces to both SDRs (b) and (c) using 4xSPF28 to QSFP28 network cables, which support high data-rate transmission of up to 100 Gbps. This elevated throughput is motivated by the ability of SDRs to handle signals with a bandwidth of up to 400 MHz, in the frequency range from 1 MHz to 7.2 GHz. As shown in Fig. 2, the signals originating from devices (b) and (c) are routed through (blue) RF cables, which connect to a Keysight PROPSIM FS16 channel emulator, labeled as (d). The channel emulator serves as the core component of the proposed testbed, as it enables the emulation of impairments characteristic of ground, aerial, and space channels, enabling both terrestrial and non-terrestrial communication scenarios. The PROPSIM FS16 is equipped with 32 RF ports, including 16 full-duplex IN/OUT interfaces and 16 half-duplex OUT-only ports. Signals from the SDRs enter the emulator through one of the IN/OUT ports, are processed according to the selected channel model, and then exit through one of the OUT ports to reach the corresponding communication endpoint. In our testbed configuration, the TX/RX ports of the gNB and UE USRPs are connected to the first through fourth interfaces of the PROPSIM, respectively. To ensure synchronization, an OctoClock-G CDA-2990, labeled (e) in Fig. 2, is used to distribute reference signals via RF cables to both SDRs, providing frequency and time alignment.

## B. Software Setup

Regarding the software components, our testbed is based on the open-source framework developed by the OAI Software Alliance, namely OpenAirInterface5G [15], hereafter referred to as OAI. This framework provides full-stack support for both 5G NG-RAN and 5G Core Network (CN) functionalities. OAI was selected due to its comprehensive support for the NTN-specific adaptations introduced by 3GPP in Release 17, as detailed in Section II-A. All 5G network nodes — namely, the CN, gNB, and UE — are implemented on the WS using the OAI framework. To construct our 5G-compliant testbed, we first deploy the core network (CN), which is built using Docker containers hosting the basis 5G network functions: User Plane Function (UPF), Access and Mobility Management Function (AMF), Session Management Function (SMF). These components collectively enable core 5G services, such as connectivity management, mobility support, session establishment, and network slicing, thereby allowing realistic and standards-compliant network emulation. The gNB and UE functionalities are realised through OAI executables, i.e., `nr-softmodem` and `nr-uesoftmodem`, respectively. Both nodes can be configured using either configuration files or command-line flags at runtime, providing full control over all relevant parameters needed to set up end-to-end connectivity between the UE and the 5G network. Furthermore, gNB and UE executables can also be deployed as Docker containers to facilitate the reproducibility of the same scenario.

To set up the emulation environment of the PROPSIM FS16, the Keysight *Geometric Channel Modeling (GCM)* tool is employed, featuring an intuitive graphical user interface that facilitates the creation of sophisticated and dynamic channel models involving mobility, multiple radio nodes, antenna arrays, and directional beam patterns. Furthermore, the tool supports the emulation of satellite links — both GEO and LEO — in transparent and regenerative modes, enabling realistic modeling of non-terrestrial communication environments. In the next section, we analyse specific uses of the GCM tool to emulate both terrestrial and non-terrestrial communications, using proper configurations of the OAI parameters and related adaptations required by the 5G standard for the NTN cases.

# IV. Experimental Results

This section presents a performance assessment of 5G TN and NTN segments, using the experimental emulation

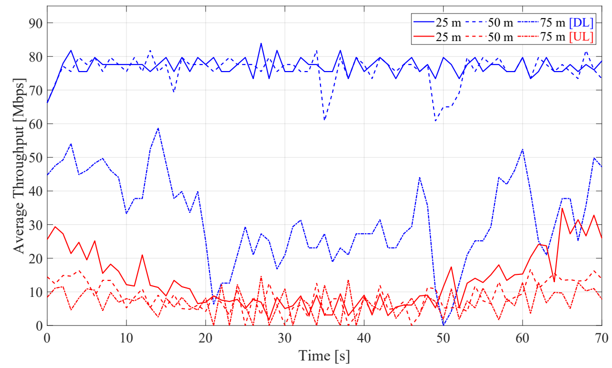


Fig. 3. Average downlink (blue) and uplink (red) throughput over time for UE–gNB horizontal distances of 25, 50, and 75 m.

capabilities of the proposed testbed, while analysing key metrics that highlight challenges and limitations arising from their integration. In our setup, NTN adaptations involve only the UE and gNB nodes; thus, both deployments share the same CN functions. Unless otherwise specified, throughput measurements are obtained creating a TCP stream through iPerf3 tool, while the RTT is evaluated via ping, with ICMP packet size shaped to control traffic bandwidth.

## A. Emulation of a TN Segment

For the TN segment, we consider a simplified yet representative outdoor scenario accounting for a gNB mounted at an altitude of $30\,\mathrm{m}$ featuring a dipole-like antenna and configured to operate within the n78 band, with a subcarrier spacing of $30\,\mathrm{kHz}$, and the overall bandwidth set to $40\,\mathrm{MHz}$ (i.e., 106 resource blocks). Moreover, uplink and downlink transmissions are scheduled according to a Time Division Duplex (TDD) scheme, in compliance with the 5G standard for the adopted frequency range. Among the available path-loss models in the emulator, we adopt the free-space channel, which takes into account the distance between the gNB and the UE as determined by the mobility patterns of the latter. Specifically, the UE mimics a mobile user following a dynamic trajectory, moving along a $100\,\mathrm{m}$ straight path parallel to the stationary gNB at three increasing distances of 25, 50, and 75 m, respectively. The UE moves at a speed of $1.4\ \mathrm{m/s}$, resulting in a total emulation time of about $70\,\mathrm{s}$. Fig. 3 shows results in terms of average downlink (in blue) and uplink (in red) throughput, computed over 5 independent emulation runs, as a function of the emulation time. As it can be seen, for the downlink case, there are no significant differences between the $25\,\mathrm{m}$ and $50\,\mathrm{m}$ cases, with throughput remaining stable for the entire duration at about $80\,\mathrm{Mbps}$. As the UE moves at a horizontal distance of $75\,\mathrm{m}$ from the gNB, the capacity of the radio link fluctuates between high and low values. Inspection of the OAI logs during the measurement phase suggests that this behavior is likely caused by continuously varying channel conditions, which hinder the adaptive modulation and coding scheme from selecting the most appropriate configuration. This is also evident when observing the uplink channel, where the throughput is counterintuitively more unstable when the free-space path loss is lower, i.e., in the middle of the UE trajectory.

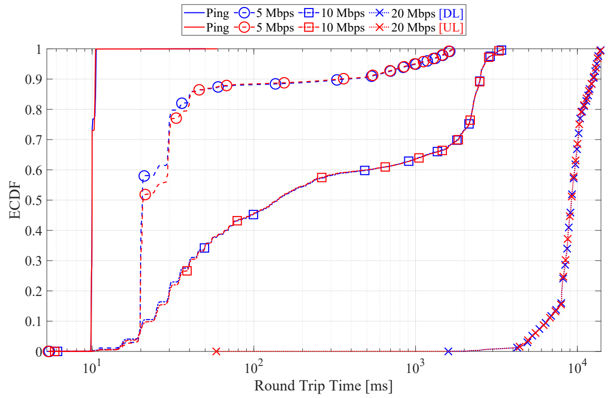

Fig. 4. ECDF of the RTT in the configuration of UE–gNB distance of 50 m by using ping (default mode and traffic loads of $\{5, 10, 20\}$ Mbps).

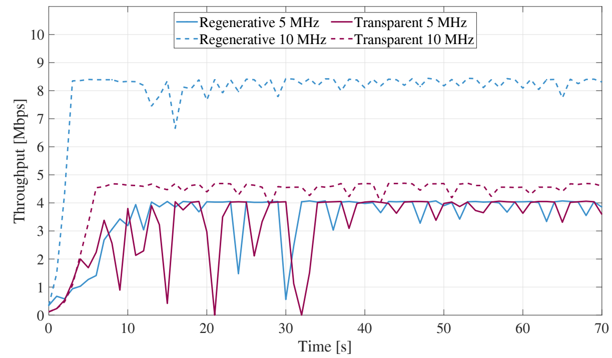

Fig. 5. Uplink throughput over time for the regenerative (cyan) and transparent (violet) mode, under $5\,\mathrm{MHz}$ and $10\,\mathrm{MHz}$ bandwidth configurations.

Moreover, throughput values are generally lower than in the downlink case due to the allocation of time resources. In fact, the adopted TDD scheme assigns 7 slots to the downlink, 2 to the uplink, and 1 to a flexible slot.

Fig. 4 shows the Empirical Cumulative Distribution Function (ECDF) of the measured RTT in the configuration with a UE-gNB distance of $50\,\mathrm{m}$. Results are reported for both uplink (red) and downlink (blue), using the standard ping tool under different traffic loads — specifically, default mode and adjusted configurations generating traffic loads of $\{5, 10, 20\}$ Mbps by tuning packet size and transmission frequency. As it can be observed, both directions experience similar performance due to non-simultaneous tests and, in turn, full bandwidth availability. More in detail, the default ping case results in a stable RTT predominantly below $10\,\mathrm{ms}$. As the traffic load increases to $5\,\mathrm{Mbps}$, the corresponding RTT slightly increases, but to only a few tens of milliseconds for 80% of the measurements. As the traffic load further increases to $10\,\mathrm{Mbps}$, about 65% of the measurements exhibit a RTT less than $1\,\mathrm{s}$, while the rest are higher but still within $2\,\mathrm{s}$, likely due to a throughput saturation phenomena. This is further evident from the $20\,\mathrm{Mbps}$ case, where the RTT ranges from few seconds up to approximately $10\,\mathrm{s}$ seconds.

## *B. Emulation of an NTN Segment*

For the NTN segment, we take into account scenarios featuring a GEO satellite and considering both transparent and regenerative modes. In the regenerative case, an ideal feeder link is assumed, implying negligible latency between the gNB and the CN. This is tantamount to considering the CN and the demanded service on-board the satellite, since the channel emulator can only reproduce the delay introduced by the radio link. In particular, the UE is located on the ground at coordinates ($0°$N, $0°$E) and communicates with a geosynchronous satellite positioned to provide an elevation angle of $90°$. In the transparent mode, the gNB lays on the ground at the same geographical coordinates of the satellite. The NTN cell adopts a Frequency Division Duplex (FDD) scheme in the n254 frequency band, with a subcarrier spacing of $15\,\mathrm{kHz}$ and the working bandwidths of $\{5, 10\}$ MHz, corresponding to 25 and 52 resource blocks, respectively.

As to the non-terrestrial channel emulation, the GCM tool provide an interface where a 5G-NTN scenario involving a GEO satellite can be created. Specifically, the NTN architecture can be set to either *Regenerative* (for the 5G regenerative case) or *Bent-Pipe* (to emulate the transparent mode).

Based on the selected configuration, the emulator automatically applies appropriate propagation delays, attenuation, and other channel-specific effects, adhering to the 3GPP technical reports [16]. In our measurement campaign, the channel was modeled as a single-tap link without fading effects.

In parallel, OAI requires manual configuration of several parameters in the UE and gNB settings to implement the NTN adaptations described in Section II-A, for which a comprehensive guide can be found in the official code repository [15].

Notably, the parameters `cellSpecificKoffset_r17` and `ta-Common-r17` are set to 478 and 58629666 for the transparent mode, and to 240 and 0 for the regenerative mode, respectively. The former refers to the scheduling offset, calculated as the number of time slots that elapse during the two-way propagation delay. The latter corresponds to twice the one-way propagation delay between the gNB and the satellite platform, computed with a time resolution of $4.072\,\mathrm{ns}$. In the regenerative configuration, these two values are effectively equivalent. As in the TN scenario, measurements were collected over an emulation period of approximately $70\,\mathrm{s}$.

Fig. 5 illustrates the trend of uplink throughput over time for both bandwidth configurations and satellite architecture configurations. The analysis starts with the uplink as it typically represents the most constrained link in a NTN deployment. At $5\,\mathrm{MHz}$, both configurations perform comparably, although the transparent mode exhibits slightly reduced stability, while the behavior differs at $10\,\mathrm{MHz}$. In the regenerative configuration, doubling the bandwidth from $5\,\mathrm{MHz}$ to $10\,\mathrm{MHz}$ yields an almost proportional increase in peak throughput. Conversely, this scaling effect is absent in the transparent mode, likely due to the substantial propagation delays impairing higher-layer retransmissions and acknowledgment mechanisms.

Figs. 6a and 6b show the ECDF of the RTT, measured using the standard ping utility in default mode, and under varying packet sizes to generate traffic loads equal to $2\,\mathrm{Mbps}$ and $5\,\mathrm{Mbps}$ for the transparent and regenerative modes, respectively. In the transparent mode, the default ping shows RTT

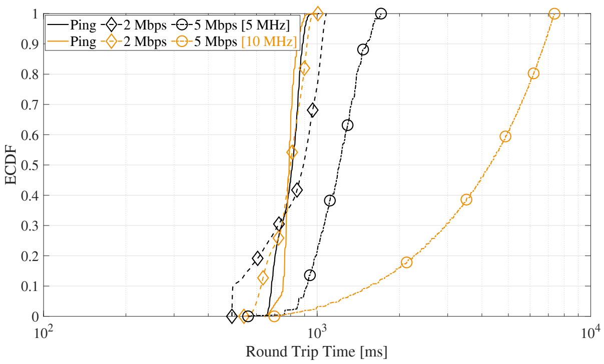


(a)

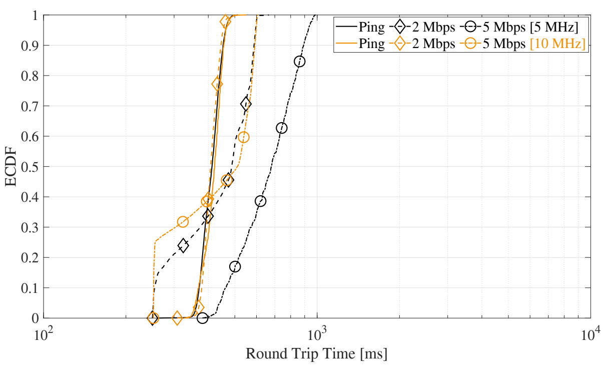


(b)

Fig. 6. ECDF of the RTT measured in the downlink direction in (a) transparent and (b) regenerative modes for 5 MHz (black) and 10 MHz (orange) by using ping (default mode and traffic loads of $\{2, 5\}$ Mbps).

values with limited variability, mostly remaining below $1\,\mathrm{s}$ for both bandwidths. At a traffic load of $2\,\mathrm{Mbps}$, still lower RTT values are achieved for the two bandwidth configurations, with only few measurements slightly exceeding $1\,\mathrm{s}$. At $5\,\mathrm{Mbps}$, the two bandwidths diverge significantly and the $10\,\mathrm{MHz}$ configuration experiences severe degradation, with RTT values reaching up to around $20\,\mathrm{s}$. In contrast, the regenerative mode maintains consistent performance across all scenarios. Both bandwidths behave similarly under default ping and quite similarly at $2\,\mathrm{Mbps}$ traffic load, while at $5\,\mathrm{Mbps}$, the $5\,\mathrm{MHz}$ configuration shows slightly higher RTT values than $10\,\mathrm{MHz}$. However, in all cases RTT values do not exceed $1\,\mathrm{s}$. These results confirm that the regenerative mode ensures stable performance across different bandwidths and traffic loads. In contrast, the transparent mode, with its inherently longer RTTs, becomes increasingly sensitive to traffic load and bandwidth scaling. Overall, these findings highlight the regenerative mode as a more robust solution for GEO-based scenarios, which will be explored further in view of the complete T/NTN integration.

## V. Conclusion

This work addresses the integration and in-lab evaluation of T/NTNs, recognised as a native feature of 6G mobile networks. The laboratory testbed, developed within the RESTART ITA-NTN project, enables the emulation of ground-, aerial-, and satellite-based links through advanced RF channel modeling. The setup combines commercial SDR, the Keysight PROPSIM FS16 channel emulator, and the OAI stack for full 5G NG-RAN and core support. The contribution preliminary explores different T/NTN scenarios, analysing key performance metrics (such as throughput and RTT) and challenges. Future work will expand the performance evaluation campaign to include 5G lower-layer metrics. Additionally, more challenging scenarios will be included, such as other elevation angles in GEO scenarios and the evaluation of LEO satellites. The latter bring several challenges, including Doppler shifts and frequent handovers.

## Acknowledgements

This work was supported by the EU under Italy NRRP (NextGenerationEU): RESTART (PE00000001, CUP: D93C22000910001), MOST (CN00000023, CUP: D93C22000410001), and SERICS (PE00000007, CUP: D33C22001300002, project ISP5G+). Additional support came from PRIN 2022 projects INSPIRE (2022BEXMXN 01) and HORUS (2022P44KA8) funded by MUR, and the HORIZON MSCA project BRIDGITISE (grant 101119554).

## References

[1] M. M. Azari, S. Solanki *et al.*, "Evolution of Non-Terrestrial Networks From 5G to 6G: A Survey," *IEEE Communications Surveys & Tutorials*, vol. 24, no. 4, pp. 2633–2672, 2022.

[2] A. Rago, A. Guidotti *et al.*, "Multi-layer NTN architectures toward 6G: The ITA-NTN view," *Computer Networks*, vol. 254, p. 110725, 2024.

[3] F. Matera, M. Settembre *et al.*, "Terrestrial and Non-Terrestrial Networks for Integrated Sensing and Communication," in *2024 IEEE International Symposium on Systems Engineering (ISSE)*, 2024, pp. 1–5.

[4] M. El Jaafari, N. Chuberre *et al.*, "Introduction to the 3GPP-defined NTN standard: A comprehensive view on the 3GPP work on NTN," *International Journal of Satellite Communications and Networking*, vol. 41, no. 3, pp. 220–238, 2023. [Online]. Available: https://onlinelibrary.wiley.com/doi/abs/10.1002/sat.1471

[5] F. Rinaldi, H.-L. Maattanen *et al.*, "Non-Terrestrial Networks in 5G & Beyond: A Survey," *IEEE Access*, vol. 8, pp. 165 178–165 200, 2020.

[6] S. Kumar, C. K. Sheemar *et al.*, "Experimental Study of the Effects of RLC Modes for 5G-NTN Applications Using OpenAirInterface5G," in *2023 IEEE Globecom Workshops (GC Wkshps)*, 2023, pp. 233–238.

[7] F. Völk, T. Schlichter *et al.*, "Field Trial of a 5G Non-Terrestrial Network Using OpenAirInterface," *IEEE Open Journal of Vehicular Technology*, vol. 3, pp. 243–250, 2022.

[8] S. Kumar, C. K. Sheemar *et al.*, "5G NTN LEO based demonstrator using OpenAirInterface5G," in *40th International Communications Satellite Systems Conference (ICSSC 2023)*, 2023, pp. 69–75.

[9] S. Kumar, A. Astro *et al.*, "5G-NTN GEO-based In-Lab Demonstrator using OpenAirInterface5G," in *11th Advanced Satellite Multimedia Conference*, 2022.

[10] F. Völk, T. Schlichter *et al.*, "5G Non-Terrestrial Networks With OpenAirInterface: An Experimental Study Over GEO Satellites," *IEEE Access*, vol. 12, pp. 155 098–155 109, 2024.

[11] S. Kumar, A. K. Meshram *et al.*, "OpenAirInterface as a platform for 5G-NTN Research and Experimentation," in *2022 IEEE Future Networks World Forum (FNWF)*, 2022, pp. 500–506.

[12] 3GPP, "Solutions for NR to support Non-Terrestrial Networks (NTN) (Release 16)," 3rd Generation Partnership Project (3GPP), Technical Report TR 38.821 V16.2.0, Mar. 2023.

[13] M. A. Jamshed, A. Kaushik *et al.*, "Non-Terrestrial Networks for 6G: Integrated, Intelligent and Ubiquitous Connectivity," *IEEE Communications Standards Magazine*, pp. 1–1, 2025.

[14] D. Pugliese, M. Quadrini *et al.*, "Integrating terrestrial and non-terrestrial networks via IAB technology: System-level design and evaluation," *Computer Networks*, vol. 253, p. 110726, 2024.

[15] OpenAirInterface, "OpenAirInterface 5G: Full-stack 5G RAN and Core Network," https://github.com/OPENAIRINTERFACE/openairinterface5g, 2024, accessed: 2025-06-12.

[16] 3GPP, "Study on New Radio (NR) to support non-terrestrial networks (Release 15)," 3rd Generation Partnership Project (3GPP), Technical Report TR 38.811 V15.4.0, Oct. 2020.